New Topological Observability Algorithm for Hybrid Power System Static State Estimation

Eduardo Resende, *Graduate Student*, Robson Pires, *Senior Member, IEEE*, and Lamine Mili, *Life Fellow, IEEE*

***Abstract*—This work presents a new topological observability algorithm to strengthen the performance of the hybrid power system static state estimation, assuming that the supervisory control and data acquisition (SCADA) and phasor measurement unit (PMU) measurements are recorded at the same time intervals. The observability of each estimated state variable is assessed by the value assigned to its least local redundancy index. The algorithm has been specifically developed to enhance the observability of an existing wide-area monitored system and exempts its expansion from critical sets and critical measurements. These objectives are achieved by building the incidence matrices of the measurements for the nodes and branches. The performance of the proposed algorithm is evaluated using the IEEE test systems and the SIN test systems of Brazilian equivalent systems.**

***Index Terms*—Power system, static state estimation, least local redundancy index, observability.**

I. Introduction

LOCAL observability assessment is important in building a reliable database. It involves determining the observability of individual buses in a power system, which is crucial to estimate the operating conditions of a power system accurately. As an open problem, many proposals on the observability problem that aim at several goals can be found in recent research works [1]-[6], to name a few. Although the proposals in [4] and [7] consider the local observability redundancy index, the latter is conceptually different from the definition presented in this work.

A hybrid observability analysis can be addressed in two ways. The first way concerns the applied algorithms, that is, topological, numerical, algebraic, or hybrid algorithms [8]-[11]. In contrast, the second way refers to its ability to deal with measurements provided by the supervisory control and data acquisition (SCADA) or information based on phasor measurement units (PMUs) fed by the wide-area measurement system (WAMS).

In this work, the proposed algorithm is hybrid in both ways, which is based on topological and algebraic algorithms. It also deals with measurements provided by SCADA and PMU, considering that both measurement channels are recorded at the same time intervals. Although the PMU placement is a critical issue demanded by several applications [2], [5], [7]-[10], [12], [13], in this work, the PMUs throughout the system have been placed anywhere, because at the state variable level, it does not matter which telemetry channels the measurements come from. Moreover, the algorithm can be used online to identify the observability status of each bus after a contingency from failures in one or both telemetry channels. The computational time for doing this task is consistent with real-time requirements.

In the literature, one can find several studies for analysis and restoration of algebraic observability that are based on both the gain matrix [14] and the Gram matrix [15]-[17]. The algebraic observability analysis algorithm used in this work is based on that in [18], whose motivation is ease of implementation and low computational cost because the incidence matrices are all unimodular. Let us recall that a unimodular matrix is a square integer matrix with determinant 1 or -1; it is invertible. The method proposed in [18] allows us to analyze the algebraic observability of a power system using a set of measurements following the occurrence of contingencies in the communication network that causes changes in the topology of the monitored power system. Note that if a monitored system is algebraically observable, it ensures that the system is topologically observable [19]; but the converse is not generally true. However, the new topological observability algorithm is based on the least local redundancy index, which mitigates the risk of algebraic observability loss. Thus, the necessary and sufficient condition for a monitoring system to be algebraically observable is the existence of an observable spanning tree (OST).

The main contribution of this paper lies in developing a new topological observability algorithm to evaluate the monitored power system based on an assigned local redundancy index for each state variable as defined in [20]. The methodology is to build a measurement digraph from the redundant measurement placement used to monitor the system. This task is performed using the complex number formulation of the state estimator because the sparsity pattern of the resul-

Manuscript received: August 28, 2024; revised: January 18, 2025; accepted: April 14, 2025. Date of CrossCheck: April 14, 2025. Date of online publication: April 25, 2025.

This work was supported in part by CAPES (Coordenação de Aperfeiçoamento de Pessoal de Nível Superior) aiming the scholarship and financial aid addressed to E. Resende.

E. Resende and R. Pires (corresponding author) are with the Institute of Electric Systems and Energy, Federal University of Itajubá, CEP 37500-903, Itajubá, Brazil (e-mail: edumarresende@unifei.edu.br; rpires@unifei.edu.br).

L. Mili is with the Electrical and Computer Engineering Department, Virginia Tech National Capital Region, Falls Church, USA (e-mail: lmili@vt.edu).

DOI: 10.35833/MPCE.2024.000951

tant incidence matrix, which is constructed by mirroring (duplicating) its columns, is equivalent to that of the Jacobian matrix in the complex domain [21].

Furthermore, the creation of the OST for power systems is built in two steps. The first step is to obtain a minimum spanning tree, considering the digraphs of measurements used for monitoring the systems. Two algorithms can be used: Prim [22] and Kruskal [23]. The standard method (dense) uses the Prim algorithm that starts from an initial vertex, traversing the adjacent vertices and choosing the vertex connected by the arc of the most negligible weight, thus generating a minimal spanning tree to the weights of each arc. On the other hand, the sparse method is based on the Kruskal algorithm, which performs an ascending sort of the weights of each arc, sequentially adding such arcs to the minimum spanning tree as long as they do not form a loop with the previous tree. In this way, a minimal spanning tree with N vertices and $N-1$ arcs is guaranteed. To this end, the single measurements for spanning tree (SMST) algorithm is developed and applied to choose different measurements stemming from each arc of the spanning tree, avoiding the repetition of existing measurements in the critical set.

To ensure the local observability regarding each state variable to be estimated, an assigned number of measurements in the fundamental set (columns of Jacobian matrix) is guaranteed through the assignment of weighted arcs concerning the following sequence of measurements: active power flow, active power injection, and voltage angle measurements for the P-δ spanning tree. Analogously, for the Q-V spanning tree, reactive power flow, reactive power injection, and voltage magnitude measurements are assigned to each fundamental set. In addition to being useful for evaluating local observability, the proposed methodology is helpful to study the expansion of monitoring systems free of critical sets of measurements.

This paper is organized as follows. Section II describes the core of the contribution proposed in this work: the new topological observability algorithm. Section III presents the numerical applications of IEEE test systems and the SIN test systems of of Brazilian equivalent systems. Section IV summarizes the main results and conclusions and outlines future investigations.

II. New Topological Observability Algorithm

In the literature, two classes of algorithms are aimed at analyzing the system observability. The first class is based on algebraic observability analysis; and the second uses graph theory and is called topological observability analysis. In this work, we develop a new topological observability algorithm based on an assigned local redundancy index of measurements around each state variable. Regardless of which telemetry channel provides the set of measurements, i.e., SCADA or WAMS, the topological observability analysis is performed considering an assigned value for the least local redundancy index.

The developed algorithm can be used to achieve two objectives. The first objective is to evaluate an existing set of measurements. All critical sets and measurements are found if they exist, including observable islands in the monitored system. The second objective is to obtain a new placement of measurements based on an assigned local redundancy index around each state variable [20]. To this end, the measurements used to monitor the system are split into the P-δ and Q-V sub-problems. In the sequel, the incidence matrices [18] for each sub-problem are built using the topology of a network system and its power flow solution. The proposed algorithm builds the set of P-δ and Q-V measurements exempted from the critical sets and critical measurements based on the full incidence matrices and the assigned local redundancy index.

A. Local Redundancy Index

Identifying weaknesses in the monitored system is carried out for each estimated state variable. This task is performed by analyzing the columns of the incidence matrix $\boldsymbol{W}_0$ for the P-δ and Q-V sub-problems $\boldsymbol{W}_{0P\text{-}\delta}$ and $\boldsymbol{W}_{0Q\text{-}V}$, respectively. The framework of these matrices is the same as the Jacobian matrix presented in [21]. The columns of the incidence matrices are referred to as the "fundamental set of measurements". These measurements play a crucial role in estimating the corresponding state variable. It is important to note that any measurement may be shared among fundamental sets, such as active and reactive power injection and voltage phase angle measurements.

The "fundamental set" concept was introduced in power system static state estimation by [24]. It is based on defining a maximum fraction of measurements contaminated by gross error. This concept ensures that the number of measurements with gross errors in each fundamental set does not violate the constraint given by:

$$f_{j,\max} \le \left\lceil \frac{m_j - 1}{2} \right\rceil \tag{1}$$

where m_j is the local redundancy index and is equal to the number of measurements of the j^{th} fundamental set Z_j; and the operator $\lceil \cdot \rceil$ denotes the integer part of its argument. Therefore, the state estimator can produce valid estimates if the constraint expressed in (1) is not violated. Consequently, let us consider that each state variable is estimated at least by an assigned minimum number of measurements, i.e., $m_j \ge \eta_{target}$. For instance, if $\eta_{target} = 3$ or 4, only one gross error in the fundamental set is possible. Otherwise, the corresponding estimated state and neighbor state variables might be unacceptable. Hence, η_{target} can now be defined as being the least local redundancy index, that is, the smallest number of measurements in any fundamental set that allows the state estimator to produce valid estimates since the constraint established in (1) is satisfied. Indeed, assigning sufficient measurements to each node in incidence matrices of P-δ and Q-V sub-problems $\boldsymbol{W}_{P\text{-}\delta}$ and $\boldsymbol{W}_{Q\text{-}V}$, which are used to construct the Jacobian matrix, ensures that the local measurement redundancy for estimating each state variable is adequate to allow an algorithm to effectively perform bad data detection and identification, i.e., detecting, identifying, down-weighting its impact on estimates, or even recovering it as a pseudo measurement.

In the sequel, Fig. 1 displays the flowchart, and Algorithm 1 shows the pseudo-code for new topological observability algorithm aimed at building a reliable database.

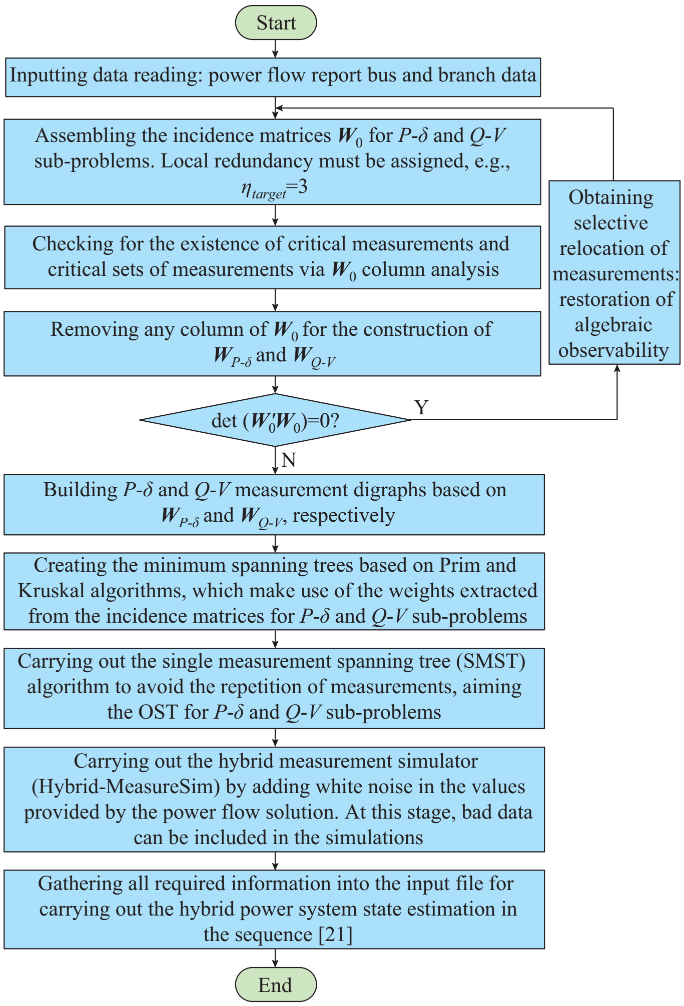

Fig. 1. Flowchart for real-time algorithm execution.

Algorithm 1: new topological observability algorithm

Input power flow data
Construct $W_{0P\text{-}\delta}$ and $W_{0Q\text{-}V}$
Set η_{target}
for $i = 1, 2, \ldots, n_{columns}$ of $W_{0P\text{-}\delta}$ and $W_{0Q\text{-}V}$ **do**
  Choose η_{target} measurements for each column of $W_{0P\text{-}\delta}$ and $W_{0Q\text{-}V}$ originating $W_{P\text{-}\delta}$ and $W_{Q\text{-}V}$
end for
for $i = 1, 2, \ldots, n_{columns}$ of $W_{P\text{-}\delta}$ and $W_{Q\text{-}V}$ **do**
  $W_{1P\text{-}\delta} \leftarrow$ remove the i^{th} column of $W_{P\text{-}\delta}$
  $W_{1Q\text{-}V} \leftarrow$ remove the i^{th} column of $W_{Q\text{-}V}$
  if $\det(W_{1P\text{-}\delta} W_{1P\text{-}\delta}^{T}) = 0$ or $\det(W_{1Q\text{-}V} W_{1Q\text{-}V}) = 0$ **then**
    System is not algebraically observable (relocation of measurements)
    Break
  else
    Continue
  end if
  For each i^{th} column of $W_{P\text{-}\delta}$ and $W_{Q\text{-}V}$, the local redundancy index and the existence of critical sets and measurements are verified
end for
Construct measurement digraphs based on $W_{P\text{-}\delta}$ and $W_{Q\text{-}V}$
Generate a minimum spanning tree applying Prim or Kruskal algorithms to measurement digraphs considering the weights extracted from incidence matrices
for $i = 1, 2, \ldots, n_{arcs}$ of each minimum spanning tree **do**
  Choose one measurement to represent the arc based on the weights of each possible measurement for that arc
  Exclude this measurement from all possible sets of measurements
end for

As an example of application, the performance of the proposed algorithm is used in the simulations carried out and presented in [21] to assess the performance of hybrid power system static state estimation.

B. Incidence Matrices for P-δ and Q-V Sub-problems

To show how the proposed algorithm works, let us first consider a small example system, as shown in Fig. 2, where t and u represent the active and reactive power flow measurements, respectively; P and Q are the active and reactive power injections, respectively; and $\dot{V}$ is the voltage phasor measurement. Hence, the full incidence matrices of measurements to nodes regarding the P-δ and Q-V sub-problems can be known, as shown in the sequence [18]. Notice that in the P-δ sub-problem (2), the voltage phase angle measurement follows the same rule of active power injection, while in the Q-V sub-problem (3), the node 0 refers to the ground potential.

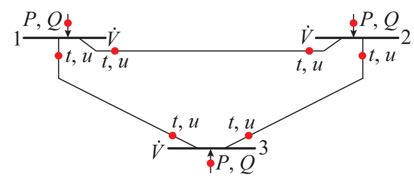

Fig. 2. Single-line diagram of 3-bus system.

$$W_{0P\text{-}\delta} = \begin{array}{c} \overbrace{\begin{array}{ccc} 1 & 2 & 3 \end{array}}^{\text{Nodes}} \\ \begin{bmatrix} 1 & -1 & 0 \\ -1 & 1 & 0 \\ 1 & 0 & -1 \\ -1 & 0 & 1 \\ 0 & 1 & -1 \\ 0 & -1 & 1 \\ 2 & -1 & -1 \\ 2 & -1 & -1 \\ -1 & 2 & -1 \\ -1 & 2 & -1 \\ -1 & -1 & 2 \\ 1 & 1 & 2 \end{bmatrix} \end{array} \left.\begin{array}{c} t_{12} \\ t_{21} \\ t_{13} \\ t_{31} \\ t_{23} \\ t_{32} \\ \delta_1 \\ P_1 \\ \delta_2 \\ P_2 \\ \delta_3 \\ P_3 \end{array}\right\} \text{Measurements} \tag{2}$$

where t_{ij} ($i, j = 1, 2, 3$ and $i \neq j$) denotes the active power flow measurement between nodes i and j; δ_i ($i = 1, 2, 3$) denotes the voltage phase angle of node i; and P_i ($i = 1, 2, 3$) denotes the active power of node i.

$$W_{0Q\text{-}V} = \begin{array}{c} \overbrace{\begin{array}{cccc} 0 & 1 & 2 & 3 \end{array}}^{\text{Nodes}} \\ \begin{bmatrix} -1 & 1 & 0 & 0 \\ -1 & 0 & 1 & 0 \\ -1 & 0 & 0 & 1 \\ 0 & 1 & -1 & 0 \\ 0 & -1 & 1 & 0 \\ 0 & 1 & 0 & -1 \\ 0 & -1 & 0 & 1 \\ 0 & 0 & 1 & -1 \\ 0 & 0 & -1 & 1 \\ 0 & 2 & -1 & -1 \\ 0 & -1 & 2 & -1 \\ 0 & -1 & -1 & 2 \end{bmatrix} \end{array} \left.\begin{array}{c} |V_1| \\ |V_2| \\ |V_3| \\ u_{12} \\ u_{21} \\ u_{13} \\ u_{31} \\ u_{23} \\ u_{32} \\ Q_1 \\ Q_2 \\ Q_3 \end{array}\right\} \text{Measurements} \tag{3}$$

where $|V_i|$ $(i=1,2,3)$ denotes the magnitude of the voltage at node i; u_{ij} $(i,j=1,2,3 \text{ and } i\neq j)$ denotes the reactive power flow measurement between nodes i and j; and Q_i $(i=1, 2, 3)$ denotes the reactive power of node i.

Additionally, in the above incidence matrices, i.e., (2) and (3), the positive values represent the emission degrees of the corresponding vertex in the P-δ and Q-V plans of measurements to be built hereafter.

Note that in (2), each fundamental set of measurements is of the same size, i.e., $m_j=10$. Whereas in (3), except for the node representative of the ground potential where $m_j=3$, which is equal to η_{target}, the size of the remaining fundamental sets is $m_j=8$.

Note that the algebraic observability makes use of the property present in the Gram matrix, $G(\boldsymbol{W})=\det|\boldsymbol{W}^{\mathrm{T}}\boldsymbol{W}|$, as follows.

$$\begin{cases}\det|\boldsymbol{W}^{\mathrm{T}}\boldsymbol{W}|\neq 0 & \text{network is observable}\\ \text{otherwise} & \text{network is not observable}\end{cases} \tag{4}$$

Note that the incidence matrix $\boldsymbol{W}$ of measurements to the nodes is also a function of two other incidence matrices given by (5). $\boldsymbol{M}$ and $\boldsymbol{A}$ for the foregoing sub-problems are defined as [18]:

$$\boldsymbol{W}=\boldsymbol{M}\boldsymbol{A}^{\mathrm{T}} \tag{5}$$

1) $\boldsymbol{M}$: Incidence Matrix of Measurements to Network Branches

$$\boldsymbol{M}_{0P\text{-}\delta}=\begin{array}{c}\overbrace{\begin{array}{ccc}1\text{-}2 & 1\text{-}3 & 2\text{-}3\end{array}}^{\text{Branches}}\\ \begin{bmatrix}1&0&0\\-1&0&0\\0&1&0\\0&-1&0\\0&0&1\\0&0&-1\\1&1&0\\1&1&0\\-1&0&1\\-1&0&1\\0&-1&-1\\0&-1&-1\end{bmatrix}\end{array}\left.\begin{array}{c}t_{12}\\t_{21}\\t_{13}\\t_{31}\\t_{23}\\t_{32}\\\delta_1\\P_1\\\delta_2\\P_2\\\delta_3\\P_3\end{array}\right\}\text{Measurements} \tag{6}$$

$$\boldsymbol{M}_{0Q-V}=\begin{array}{c}\overbrace{\begin{array}{cccccc}1\text{-}2 & 1\text{-}3 & 2\text{-}3 & 1\text{-}0 & 2\text{-}0 & 3\text{-}0\end{array}}^{\text{Branches}}\\ \begin{bmatrix}0&0&0&1&0&0\\0&0&0&0&1&0\\0&0&0&0&0&1\\1&0&0&0&0&0\\-1&0&0&0&0&0\\0&1&0&0&0&0\\0&-1&0&0&0&0\\0&0&1&0&0&0\\0&0&-1&0&0&0\\1&1&0&0&0&0\\-1&0&1&0&0&0\\0&-1&-1&0&0&0\end{bmatrix}\end{array}\left.\begin{array}{c}|V_1|\\|V_2|\\|V_3|\\u_{12}\\u_{21}\\u_{13}\\u_{31}\\u_{23}\\u_{32}\\Q_1\\Q_2\\Q_3\end{array}\right\}\text{Measurements} \tag{7}$$

2) $\boldsymbol{A}$: Incidence Matrix of Nodes to Network Branches

$$\boldsymbol{A}_{0P\text{-}\delta}=\begin{array}{c}\overbrace{\begin{array}{ccc}1\text{-}2 & 1\text{-}3 & 2\text{-}3\end{array}}^{\text{Branches}}\\ \begin{bmatrix}1&1&0\\-1&0&1\\0&-1&-1\end{bmatrix}\end{array}\left.\begin{array}{c}1\\2\\3\end{array}\right\}\text{Nodes} \tag{8}$$

$$\boldsymbol{A}_{0Q\text{-}V}=\begin{array}{c}\overbrace{\begin{array}{cccccc}1\text{-}2 & 1\text{-}3 & 2\text{-}3 & 1\text{-}0 & 2\text{-}0 & 3\text{-}0\end{array}}^{\text{Branches}}\\ \begin{bmatrix}0&0&0&-1&-1&-1\\1&1&0&1&0&0\\-1&0&1&0&1&0\\0&-1&-1&0&0&1\end{bmatrix}\end{array}\left.\begin{array}{c}0\\1\\2\\3\end{array}\right\}\text{Nodes} \tag{9}$$

The primary motivation for using the above incidence matrices is that both of them are unimodular arrays. They are matrices made up of integers or multiples equal to 1, −1, and 0. In addition, they are sparse matrices that are easy to build and do not suffer from numerical instability.

Now, let us find the set of measurements for the P-δ and Q-V sub-problems exempt from critical sets and critical measurements, including an assigned local redundancy index. The criterion for choosing the local redundancy index is explained next.

C. Building Full Measurement Plans for P-δ and Q-V

Obtaining the P-δ and Q-V sets of measurements is done independently. In this sense, the starting node (fundamental set) may be random, including choosing η_{target} measurements among $m_j=10$ measurements available in the P-δ incidence matrix. The same reasoning may be applied to the Q-V incidence matrix, where $m_j=8$.

After the first one has been analyzed, the processing of each fundamental set of measurements must obey the following necessary rule: whatever the η_{target} measurements are chosen in the first fundamental set, if any other fundamental set either totally or partially shares them, they have to be taken into account with respect to the assigned least local redundancy index, e.g., $\eta_{target}=3$.

Before continuing, it is worth remembering that in graph theory, a graph is termed a digraph when the edges are directed, which in turn is termed as arc [25]. This representation allows us to identify the emitter and receiver vertices, which are directly in line with the measurement placement of power flow, injected power, voltage phase angle, and voltage magnitude. Based on that, the digraph generated for each measurement placement can be obtained from the analysis of the matrices defined in (2) and (3). For this, consider a graph $\boldsymbol{G}_r=[\underline{\boldsymbol{a}}, \underline{\boldsymbol{b}}]$, where $\underline{\boldsymbol{a}}$ and $\underline{\boldsymbol{b}}$ are the vectors with the emitter and receiver vertices that form the arcs of the digraph, respectively. The logic elaborated for the creation of the digraphs from the incidence matrices $\boldsymbol{W}_0$ obeys the assembly rules of the vectors as follows.

1) Each bus in the electrical network corresponds to a vertex in the digraph of measurements.

2) For power flow measurements from buses k to m, the sender vertex is k and the receiver vertex is m. For the reverse power flow measurements, the sender vertex is m, and the receiver vertex is k.

3) For power injection measurements on the k^{th} bus, the positive value of the row relative to that measurement indicates the number of repetitions of the emitter vertex k, and the columns of the other non-zero elements of that row indicate the respective receiver vertices.

4) For the angular state measurements, the rule is the same as applied for power injection measurements.

5) For voltage magnitude measurements on the k^{th} bus, the emitter vertex is k, and the receiver vertex is 0.

Consequently, the full digraphs for P-δ and Q-V sub-problems can be obtained, yielding:

$$\boldsymbol{G}_{rP\text{-}\delta}=\begin{array}{cl}\begin{bmatrix}1&2\\1&3\\2&1\\2&3\\3&1\\3&2\\1&2\\1&3\\2&1\\2&3\\3&1\\3&2\\1&2\\1&3\\2&1\\2&3\\3&1\\3&2\end{bmatrix} & \begin{array}{l}\rightarrow t_{12}\\\rightarrow t_{13}\\\rightarrow t_{21}\\\rightarrow t_{23}\\\rightarrow t_{31}\\\rightarrow t_{32}\\\rightarrow P_1\\\rightarrow P_1\\\rightarrow P_2\\\rightarrow P_2\\\rightarrow P_3\\\rightarrow P_3\\\rightarrow \delta_1\\\rightarrow \delta_1\\\rightarrow \delta_2\\\rightarrow \delta_2\\\rightarrow \delta_3\\\rightarrow \delta_3\end{array}\end{array} \tag{10a}$$

$$\boldsymbol{G}_{rQ\text{-}V}=\begin{array}{cl}\begin{bmatrix}1&0\\2&0\\3&0\\1&2\\1&3\\2&1\\2&3\\3&1\\3&2\\1&2\\1&3\\2&1\\2&3\\3&1\\3&2\end{bmatrix} & \begin{array}{l}\rightarrow |V_1|\\\rightarrow |V_2|\\\rightarrow |V_3|\\\rightarrow u_{12}\\\rightarrow u_{13}\\\rightarrow u_{21}\\\rightarrow u_{23}\\\rightarrow u_{31}\\\rightarrow u_{32}\\\rightarrow Q_1\\\rightarrow Q_1\\\rightarrow Q_2\\\rightarrow Q_2\\\rightarrow Q_3\\\rightarrow Q_3\end{array}\end{array} \tag{10b}$$

In the above equation, we recall the positive impact of measurements of the angular state in the P-δ sub-problem. In the Q-V sub-problem, the number of voltage magnitude measurements ensures the vertex representative of the ground potential observability. Figures 3 and 4 show the full measurement plans for the P-δ and Q-V sub-problems, respectively. However, the corresponding measurement digraphs of P-δ and Q-V sub-problems, considering $\eta_{target}=3$, are shown in Figs. 5 and 6, respectively. It can be observed that for each vertex in Figs. 5 and 6, there are at least $\eta_{target}=3$ different measurements.

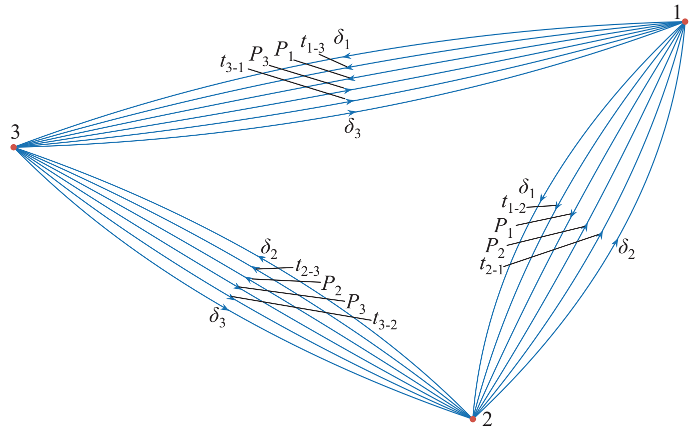

Fig. 3. Full measurement plan for P-δ sub-problem.

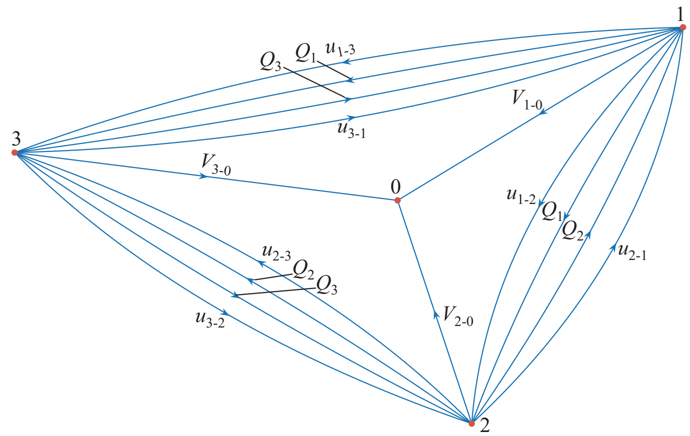

Fig. 4. Full measurement plan for Q-V sub-problem.

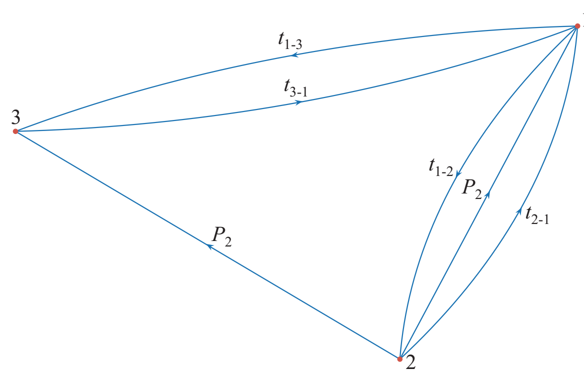

Fig. 5. Measurement digraphs of P-δ sub-problem considering $\eta_{target}=3$.

D. OST for P-δ and Q-V Sub-problems

The search for an OST for the P-δ and Q-V sub-problems is done by making use of three algorithms, i.e., Prim [22], Kruskal [23], and SMST. The Prim and Kruskal algorithms search for the minimum spanning tree, whereas the SMST algorithm finds the OST for the P-δ and Q-V sub-problems.

Prim algorithm (dense) starts from a random initial vertex connected by the arc of the most negligible weight, thus generating a minimal spanning tree about the weights of each arc. Recall that the positive value at each row in the incidence matrices of the measurements for the network nodes in (2) and (3) represents the number of arcs emitted from the node (emission degree) due to the corresponding measurement, hence, each emission degree in (2) and (3) is used as the weight assigned to the arcs referred to each measurement in the spanning tree. For instance, the weight assigned to each power flow measurement is 1. In contrast, the weight is usually 2 or more for power injection, depending on the number of incident branches converging toward the node where the power injection is measured. Furthermore, since the measurement of the angular state follows the same rule as applied to power injection, a first consideration in the construction of the spanning tree, since it is a measurement of the variable state, is to take its weight as a fraction of the actual weight, e. g., 90%. This strategy reduces its weight to less than the weight of the power injection measurement.

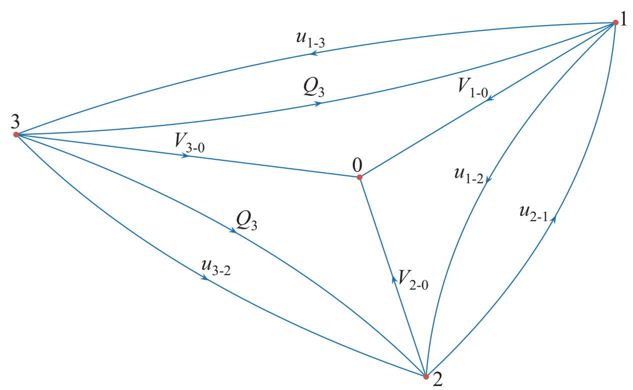

Fig. 6. Measurement digraphs of Q-V sub-problem considering $\eta_{target}=3$.

On the other hand, the sparse method is based on Kruskal algorithm, which performs an ascending sort of weights for each arc, sequentially adding such arcs to the minimum spanning tree as long as they do not form a loop with the previous tree.

At this stage, the SMST is carried out to obtain the OST once it avoids the loop formation and ensures different measurements in the minimum spanning tree. For example, Tables I and II present the OST obtained for the P-δ and Q-V sub-problems based on the Prim and Kruskal algorithms [22], [23] under the supervision of SMST algorithm, respectively. Note that the weight for each measurement is indicated by appending (1) and (2) to the arc specification.

TABLE I
OST Obtained for P-δ Sub-problem

Spanning tree arc	Set of measurement	Randomly chosen measurement
1-2	$t_{1\text{-}2}$ (1), $t_{2\text{-}1}$ (1), P_2 (2)	$t_{1\text{-}2}$
1-3	$t_{1\text{-}3}$ (1), $t_{3\text{-}1}$ (1)	$t_{1\text{-}3}$

Recall that the chosen measurements for the composition of OST are selected following the ascending order of the weight assigned to each type of measurement under the supervision of SMST algorithm. For instance, for the P-δ sub-problem, the order is power flow → angular state measurements →power injection measurements. In contrast, for the Q-V sub-problem, the order is voltage magnitude measurement → power flow → power injection measurements.

TABLE II
OST Obtained for Q-V Sub-problem

Spanning tree arc	Set of measurement	Randomly chosen measurement
1-2	$u_{1\text{-}2}$ (1) $u_{2\text{-}1}$ (1)	$u_{1\text{-}2}$
1-3	$u_{1\text{-}3}$ (1) Q_3 (2)	$u_{1\text{-}3}$
1-0	$V_{1\text{-}0}$ (1)	
2-0	$V_{2\text{-}0}$ (1)	$V_{2\text{-}0}$
3-0	$V_{3\text{-}0}$ (1)	

Note that in Figs. 7 and 8, all vertices are connected to each other. Otherwise, the corresponding measurement placement is not topologically observable.

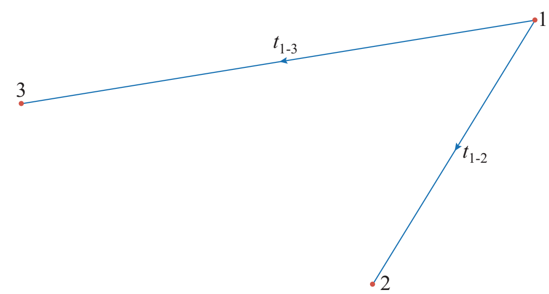

Fig. 7. OST for P-δ sub-problem.

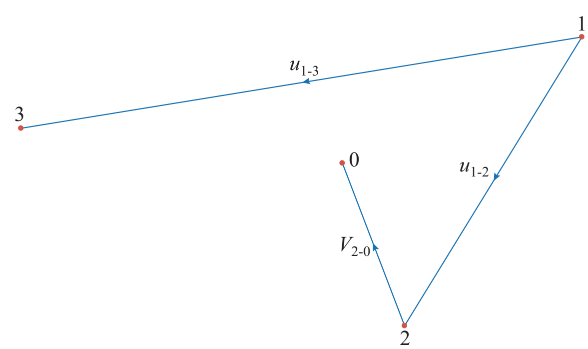

Fig. 8. OST for Q-V sub-problem.

III. Numerical Applications

This section presents the main network features and the monitored quantities for the larger-scale systems used in the simulations. The SMST algorithm was developed in MATLAB using sparsity techniques and performed on an Intel(R) Core(TM) i7-10510U CPU (@ 1.80 GHz, up to 2.30 GHz), 16 GB RAM, and 64-bit operating system. Table III depicts the power flow parameters for IEEE and SIN test systems, where N_{PV} is the number of P-V buses; N_{PQ} is the number of P-Q buses; $\boldsymbol{CV}_r$ is the complex-valued Jacobian matrix in rectangular coordinates and its dimension $n=2(N_{PV}+N_{PQ})$; and $\boldsymbol{RV}_p$ is the real-valued Jacobian matrix in polar coordinates and its dimension $n=N_{PV}+2N_{PQ}$. In contrast, Table IV presents the SMST performance considering several scenarios of measurements provided by the SCADA and PMUs.

TABLE III
POWER FLOW PARAMETERS FOR IEEE AND SIN TEST SYSTEMS

Test system	N_{PV}	N_{PQ}	No. of transformer	No. of transmission line and shunt device	n for $\boldsymbol{RV}_p$	n for $\boldsymbol{CV}_r$
IEEE 57-bus	6	50	15	83	106	112
SIN-340	53	287	82	550	627	680
SIN-730	104	626	234	1078	1356	1460
SIN-1916	163	1753	835	3197	3669	3832

TABLE IV
SMST PERFORMANCE CONSIDERING $\eta_{target}=3$

Test system	SCADA		PMU		A (s)	B (s)	
	N_m	R (%)	N_m	R (%)		P-δ	Q-V
IEEE 57-bus	239	100	-	0	0.0453	0.0132	0.0126
	185	75	27	25	0.0484	0.0136	0.0141
	120	50	60	50	0.0584	0.0129	0.0114
	59	25	91	75	0.0559	0.0122	0.0126
	-	0	121	100	0.0504	0.0131	0.0121
SIN-340	1427	100	-	0	0.2822	0.1052	0.1025
	1067	75	180	25	0.3521	0.1797	0.2564
	710	50	359	50	0.3355	0.1048	0.0972
	367	25	531	75	0.3645	0.1648	0.1877
	-	0	715	100	0.3955	0.1664	0.1838
SIN-730	3417	100	-	0	0.6898	0.6125	0.4253
	2559	75	429	25	0.6822	0.3612	0.3469
	1720	50	849	50	0.7878	0.6269	0.4538
	859	25	1280	75	0.7727	0.5036	0.4727
	-	0	1710	100	0.7675	0.4844	0.4517
SIN-1916	8453	100	-	0	2.4401	1.9982	1.8671
	6287	75	1083	25	1.8205	1.7203	1.7626
	4220	50	2117	50	1.9887	2.1164	1.9822
	2095	25	3180	75	1.9419	2.0569	1.9009
	-	0	4228	100	1.7991	1.7334	1.7511

Note: A denotes the total time for searching the critical sets and critical measurements; B denotes the time for obtaining an OST; N_m denotes the number of measurements; and R denotes the percentage of the number of measurements by the measurement devices in the total number of measurements.

When measurement noise is present in SCADA or PMUs, the impact of SMST performance is described in [21], in which results are obtained under various scenarios, assuming $\eta_{target}=3$. Furthermore, Figs. 9-12 show the comparative performance of the SMST algorithm for the most representative test systems considering different least local redundancy indices of measurements, e.g., $\eta_{target}=3$ and $\eta_{target}=5$, in P-δ and Q-V sub-problems. The least local redundancy index of the measurements has a low impact on SMST performance. Still, it positively impacts the robustness of a highly robust state estimator, as it can handle two bad data if $\eta_{target}=5$ is assigned to each fundamental set.

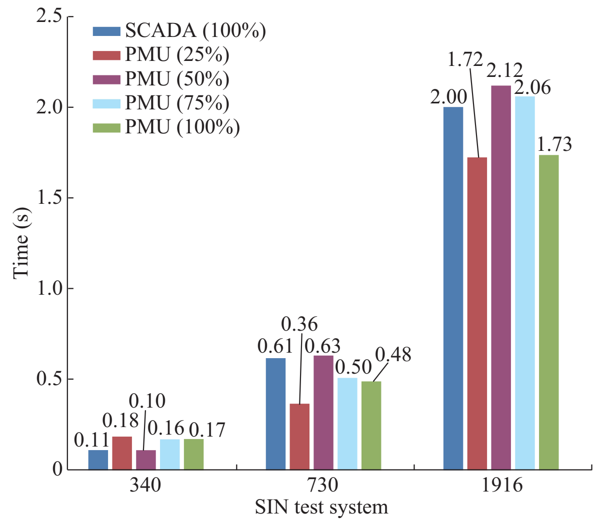

Fig. 9. P-δ sub-problem considering $\eta_{target}=3$ under SIN test systems.

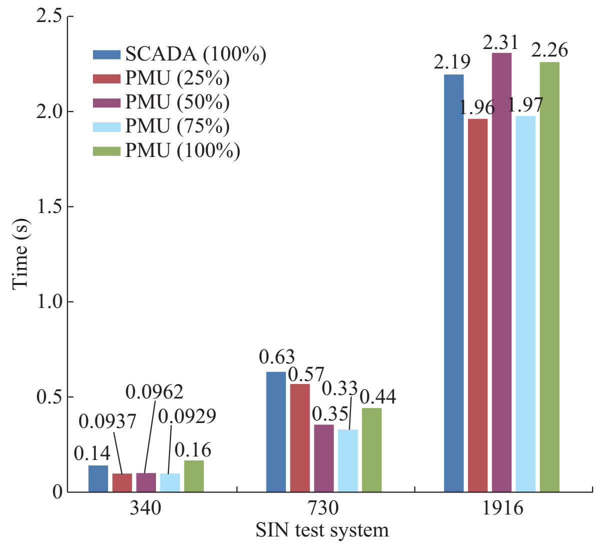

Fig. 10. P-δ sub-problem considering $\eta_{target}=5$ under SIN test systems.

On the other hand, the measurement digraphs and OSTs for the P-δ and Q-V sub-problems for larger-scale systems, considering $\eta_{target}=3$, are shown in Supplementary Material A Figs. SA1 and SA2 and in Figs. 13 and 14, respectively. Note that in both digraphs of measurements, the vertices show up with at least three ($\eta_{target}=3$) arcs converging to them, e.g., vertices #33 and #35, among others. Furthermore, for much larger-scale systems, the following functionality is useful to see the overall local redundancy for the P-δ and Q-V sub-problems, as shown in Figs. 15 and 16, respectively. Note that the IEEE 57-bus test system is chosen for illustration since much larger-scale systems cause visual pollution in the pictures due to the density of digraph connections.

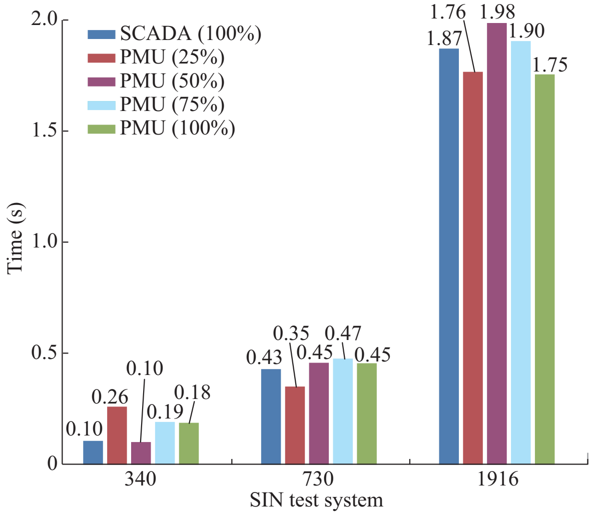

Fig. 11. Q-V sub-problem considering $\eta_{target}=3$ under SIN test systems.

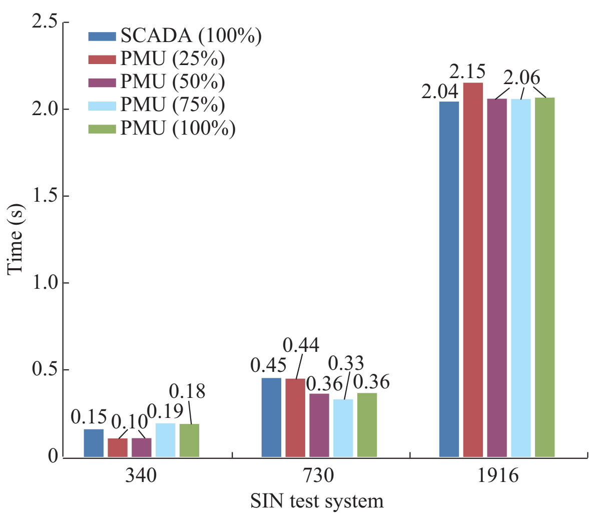

Fig. 12. Q-V sub-problem considering $\eta_{target}=5$ under SIN test systems.

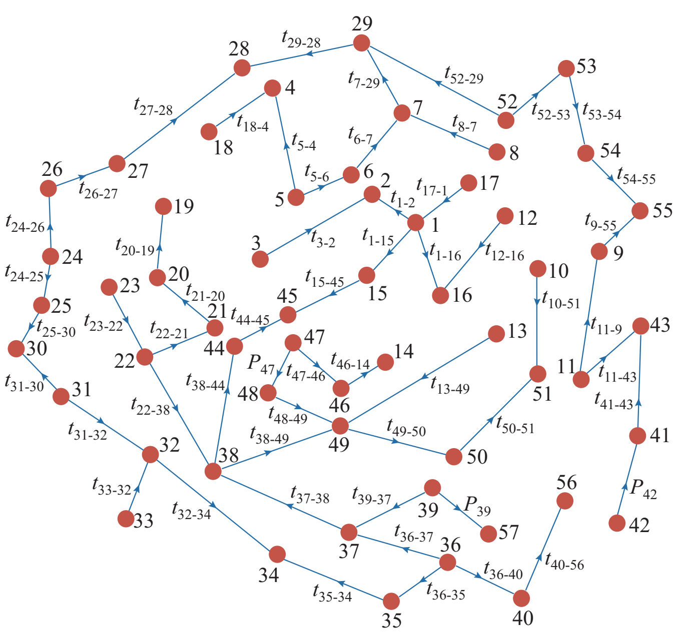

Fig. 13. OST for P-δ sub-problem applied to IEEE 57-bus test system.

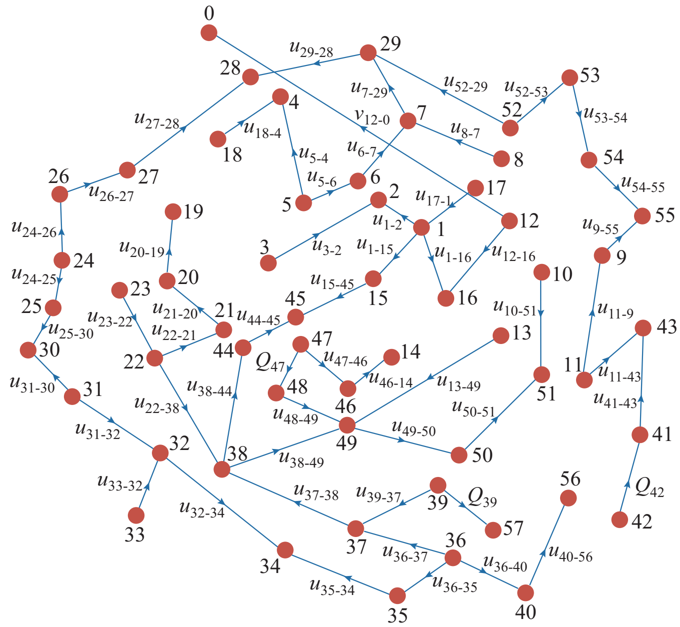

Fig. 14. OST for Q-V sub-problem applied to IEEE 57-bus test system.

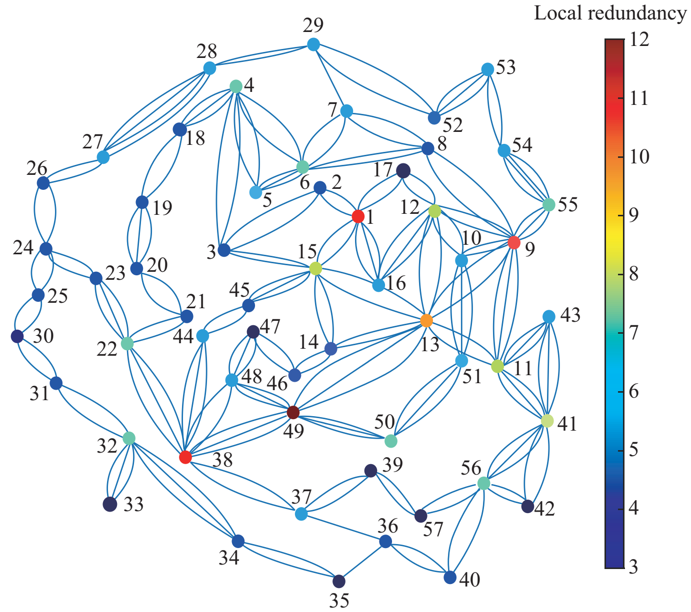

Fig. 15. Local redundancy for P-δ sub-problem under IEEE 57-bus test system.

IV. Conclusion and Future Investigation

This paper presents an algorithm of low computational cost for analyzing topological observability based on an assigned local redundancy index. Such features result from unimodular matrices obtained by the topological analysis of the network and the established real-time monitoring plan. These, known as incidence matrices, are sparse and easy to build, and do not have the risk of numerical instability. Furthermore, these matrices can be easily converted to computational applications based on graph theory, encouraging the elaboration of measurement digraphs for P-δ and Q-V sub-problems.

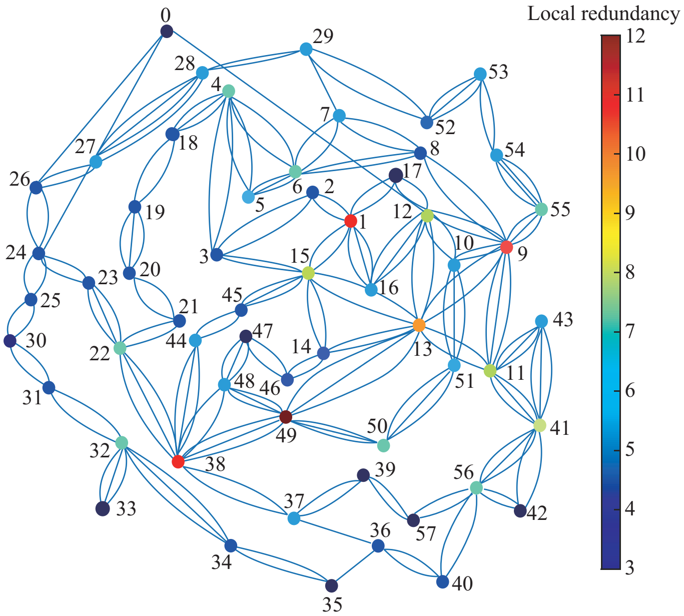

Fig. 16. Local redundancy for Q-V sub-problem under IEEE 57-bus test system.

Moreover, such applications are the basis for searching for OSTs, which is a necessary and sufficient condition to ensure topological observability. The Prim and Kruskal algorithms create spanning trees based on a given measurement digraph. A new algorithm is developed to avoid duplicity of measurement and loop formation when constructing the spanning tree. Therefore, this algorithm allows the creation of OSTs for the P-δ and Q-V sub-problems, avoiding a high computational effort since it belongs to a combinatorial problem.

Future investigations could involve developing an algorithm to create a monitoring plan that considers local redundancy depending on operational requirements. This can be done by assigning larger weights to power injection measurements, e.g., zero injection buses, since this strategy provides more arcs in the measurement digraph, ensuring algebraic observability.

References

[1] M. Z. Islam, Y. Lin, V. M. Vokkarane *et al.*, "Observability-aware resilient PMU networking," *IEEE Transactions on Power Systems*, vol. 40, no. 1, pp. 218-230, Jan. 2025.

[2] N. P. Theodorakatos, R. Babu, and A. P. Moschoudis, "The branch-and-bound algorithm in optimizing mathematical programming models to achieve power grid observability," *Axioms*, vol. 12, no. 11, p. 1040, Nov. 2023.

[3] C. Ren, X. Wang, C. Cao *et al.*, "Power systems observability analysis based on parallel Gaussian belief propagation," in *Proceedings of 2022 IEEE 10th International Conference on Computer Science and Network Technology*, Dalian, China, Oct. 2022, pp. 19-23.

[4] E. O. Okendo, C. W. Wekesa, and M. J. Saulo, "Optimal placement of phasor measurement unit considering system observability redundancy index: case study of the Kenya power transmission network," *Heliyon*, vol. 7, no. 7, p. e07670, Jul. 2021.

[5] G. N. Korres, "An integer-arithmetic algorithm for observability analysis of systems with SCADA and PMU measurements," *Electric Power Systems Research*, vol. 81, no. 7, pp. 1388-1402, Jul. 2011.

[6] M. Shahraeini and M. H. Javidi, "A survey on topological observability of power systems," in *Proceedings of 2011 IEEE Power Engineering and Automation Conference*, Wuhan, China, Sept. 2011, pp. 373-376.

[7] D. Dua, S. Dambhare, R. K. Gajbhiye *et al.*, "Optimal multistage scheduling of PMU placement: an ILP approach," *IEEE Transactions on Power Delivery*, vol. 23, no. 4, pp. 1812-1820, Oct. 2008.

[8] N. P. Theodorakatos, R. Babu, C. A. Theodoridis *et al.*, "Mathematical models for the single-channel and multi-channel PMU allocation problem and their solution algorithms," *Algorithms*, vol. 17, no. 5, p. 191, May 2024.

[9] M. Korkali, *Robust Wide-area Fault Visibility and Structural Observability in Power Systems with Synchronized Measurement Units*. New York: IEEE Press, 2020.

[10] G. N. Korres, N. M. Manousakis, T. C. Xygkis *et al.*, "Optimal phasor measurement unit placement for numerical observability in the presence of conventional measurements using semi-definite programming," *IET Generation, Transmission & Distribution*, vol. 9, no. 15, pp. 2427-2436, Dec. 2015.

[11] H. Zhang and K. Han, "A hybrid observability analysis method for power system state estimation," *IEEE Access*, vol. 8, pp. 73388-73397, Apr. 2020.

[12] T. L. Baldwin, L. Mili, M. B. Boisen *et al.*, "Power system observability with minimal phasor measurement placement," *IEEE Transactions on Power Systems*, vol. 8, no. 2, pp. 707-715, May 1993.

[13] L. Mili, T. Baldwin, and R. Adapa, "Phasor measurement placement for voltage stability analysis of power systems," in *Proceedings of 29th IEEE Conference on Decision and Control*, Honolulu, USA, Dec. 1990, pp. 3033-3038.

[14] A. Monticelli and F. F. Wu, "Network observability: identification of observable islands and measurement placement," *IEEE Transactions on Power Apparatus and Systems*, vol. 104, no. 5, pp. 1035-1041, May 1985.

[15] M. C. Almeida, E. N. Asada, and A. V. Garcia, "A numerical method for finding spanning trees in power system state estimation," in *Proceedings of 2006 International Conference on Power System Technology*, Chongqing, China, Oct. 2006, pp. 1-6.

[16] M. C. de Almeida, E. N. Asada, and A. V. Garcia, "On the use of gram matrix in observability analysis," *IEEE Transactions on Power Systems*, vol. 23, no. 1, pp. 249-251, Feb. 2008.

[17] G. N. Korres, "A gram matrix-based method for observability restoration," *IEEE Transactions on Power Systems*, vol. 26, no. 4, pp. 2569-2571, Nov. 2011.

[18] E. D. Crainic, X. D. Do, P. J. Lagacé *et al.*, "Power system observability: on-line measurement set contingency analysis," *IFAC Proceedings Volumes*, vol. 21, no. 11, pp. 491-499, Sept. 1988.

[19] G. R. Krumpholz, K. A. Clements, and P. W. Davis, "Power system observability: a practical algorithm using network topology," *IEEE Transactions on Power Apparatus and Systems*, vol. 99, no. 4, pp. 1534-1542, Jul. 1980.

[20] L. Mili, V. Phaniraj, and P. J. Rousseeuw, "Least Median of squares estimation in power systems," *IEEE Transactions on Power Systems*, vol. 6, no. 2, pp. 511-523, May 1991.

[21] E. M. Resende, R. Pires, and L. Mili, "Complex-valued projection statistics for hybrid power system state estimation," *IEEE Transactions on Power Systems*, vol. 39, no. 4, pp. 6052-6062, Jul. 2024.

[22] GeekforGeeks. (2021, Jan.). Prim's minimum spanning tree (MST)-greedy algo-5. [Online]. Available: https://www. geeksforgeeks. org/ prims-minimum-spanning-tree-mst-greedy-algo-5

[23] GeekforGeeks. (2021, Jan.). Kruskal's minimum spanning tree algorithm-greedy algo-2. [Online]. Available: https://www. geeksforgeeks. org/ kruskals-minimum-spanning-tree-algorithm-greedy-algo-2/

[24] L. Mili, V. Phaniraj, and P. J. Rousseeuw, "High breakdown point estimation in electric power systems," in *Proceedings of IEEE International Symposium on Circuits and Systems*, New Orleans, USA, May 1990, pp. 1843-1846.

[25] R. Diestel, *Graph Theory*. Heidelberg: Springer-Verlag, 2017, pp. 59-172.

Eduardo Resende received the B.Sc. degree and the M.Sc. degree in electrical engineering from Federal University of Itajuba (UNIFEI), Itajuba, Brazil, in 2020 and 2021, respectively. Since 2022, he has been working to pursue the Ph.D. degree at the Institute of Electric Systems and Energy (ISEE) at UNIFEI. His research interests include computer technologies applied to power system analysis, operation, and control.

Robson Pires received the B.Sc, M.Sc., and D.Sc. degrees in electrical engineering from Fluminense Federal University (UFF), Niterói, Brazil, Federal University of Itajuba (UNIFEI), Itajuba, Brazil, and Federal University of

Santa Catarina (UFSC), Florianópolis, Brazil, respectively. In Jan.-Jul. 1996, he did part of his graduate program at "The Bradley Department of Electrical and Computer Engineering" of Virginia Tech, Blacksburg, USA. Since 1987, he has been with the Institute of Electric Systems and Energy at UNIFEI, where he is currently a Professor. His research interests include power system analysis, real-time wide-area measurement system (WAMS) control, and complex-valued network application.

Lamine Mili is currently a Professor and the Program Director of the Department of Electrical and Computer Engineering, Northern Virginia Center, Virginia Tech, Blacksburg, USA. He was a Visiting Professor with the Swiss Federal Institute of Technology Lausanne, Lausanne, Switzerland; the Grenoble Institute of Technology, Grenoble, France, École supérieure d'électricité, Parice, France, and École Polytechnique de Tunisie, La Marsa, Tunisia. His research interests include robust estimation and control, robust Kalman filtering, copula index, risk management of complex system under catastrophic failure, non-linear dynamics, and bifurcation theory.